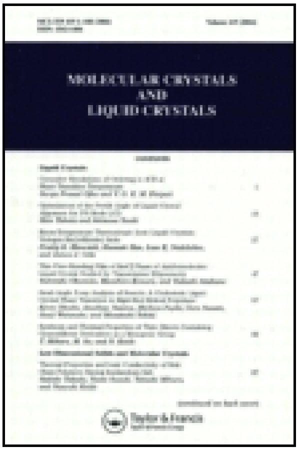

Molecular Crystals and Liquid Crystals
Publication details, including instructions for authors and subscription information:
http://www.tandfonline.com/loi/gmcl18

Nonlinear Optical Response in Ferroelectric Liquid Crystal

Masanori Ozaki [a] , Akira Tagawa [a] , Takashi Hatai [a] , Yutaka Sadohara [a] , Yutaka Ohmori [a] & Katsumi Yoshino [a]

[a] Department of Electronic Engineering, Faculty of Engineering, Osaka University, 2-1 Yamada-Oka, Suita, Osaka, Japan

Version of record first published: 24 Sep 2006.

To cite this article: Masanori Ozaki , Akira Tagawa , Takashi Hatai , Yutaka Sadohara , Yutaka Ohmori & Katsumi Yoshino (1991): Nonlinear Optical Response in Ferroelectric Liquid Crystal, Molecular Crystals and Liquid Crystals, 199:1, 213-221

To link to this article: http://dx.doi.org/10.1080/00268949108030932

Mol. Cryst. Liq. Cryst., 1991, Vol. 199, pp. 213–221
Reprints available directly from the publisher
Photocopying permitted by license only

Printed in the United States of America

Nonlinear Optical Response in Ferroelectric Liquid Crystal

MASANORI OZAKI, AKIRA TAGAWA, TAKASHI HATAI, YUTAKA SADOHARA, YUTAKA OHMORI and KATSUMI YOSHINO

Department of Electronic Engineering, Faculty of Engineering, Osaka University, 2-1 Yamada-Oka, Suita, Osaka Japan

(Received July 26, 1990)

Hybrid optical bistability and limiting using the DHS and SSFLC electro-optical effects in ferroelectric liquid crystal with linear feedback have been studied. Optical limiting and bistability are observed for the cases of negative and positive feedback parameters, respectively. It is also found that the hysteresis in the transmission-voltage curve of ferroelectric liquid crystal contributes to the expansion of the bistable region. Dynamic properties of switching between optical bistable states by the pulse incident light has also been studied.

Keywords: ferroelectric liquid crystal, liquid crystal, optical bistability, optical limiting, nonlinear optical effect

1. INTRODUCTION

Nonlinear optical responses such as optical limiting, optical amplification and optical bistability have attracted considerable attention from practical points of view as optical processing. For the realization of optical bistability, nonlinearity and feedback are required. The device whose feedback can be optically achieved by mirrors is all-optical bistability, whereas one which requires external feedback such as an electrical circuit is known as hybrid optical bistability.

In liquid crystals, mainly in nematic liquid crystals, the nonlinear optical response has also been studied.[1–3] On the other hand, the ferroelectric liquid crystal (FLC) has recently been developed as a material for high-speed display devices. In this compound, several types of electro-optical effects have been reported.[4–7] Among them the simplest electro-optical effect is deformation of helical structure (DHS) which utilizes a change of light scattering due to the transition between winding and unwinding states of the helical structure.[4,8] This effect has been reported as the first electro-optical effect in FLC.[4] The other electro-optical effect was realized with homogeneously aligned thin (less than several μm in thickness) FLC cell which was set between two polarizers and confirmed to exhibit fast response time.[5] This type of thin cell device was systematically studied by Clark and Lagerwall and named as surface stabilized ferroelectric liquid crystal (SSFLC), which has attracted much interest because of the potential application to fast electro-optical switching device.[6] In both effects, a hysteresis loop was observed in the voltage dependence of the transmission intensity.[8,9]

In this paper, the hybrid optical bistability and limiting in FLC utilizing a DHS and SSFLC cell with linear feedback are reported. Dynamic properties of switching between two stable states are also studied.

2. EXPERIMENTAL

The experimental setup for the measurement of the nonlinear response is shown in Figure 1. The light source was a He-Ne laser (632.8 nm). The transmitted light intensity through a cell was monitored with a photodiode. The output voltage was amplified, summed with a bias voltage and fed back to the sample cell.

The FLC used in this study was *p*-decyloxybenzylidene-*p*′-amino-2-methylbutylcinnamate (DOBAMBC) and a mixture liquid crystal which shows the Sm C* phase in room temperature. The sample was sandwiched between two In Sn oxide (ITO) coated conducting glass plates. The DHS cell had no special surface treatment and no polarizers, whose cell gap was determined by the thickness of the polyethyleneterephthalate sheets to be about 50 μm. In this geometry, the smectic layer was perpendicular to the cell surfaces (homogeneous alignment). For the SSFLC cell a 2 μm thick homogeneously aligned sample was prepared by rubbing after coating the surface with a polyvinylalcohol.

3. RESULTS AND DISCUSSION

3.1 Feedbacked DHS

Voltage dependence of the transmission intensity of the light through the DHS cell of DOBAMBC is shown in Figure 2(a). In the absence of field the transmission intensity is low due to the light scattering by the helical structure. With increasing

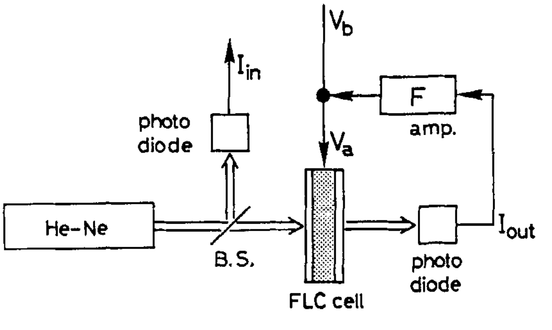

FIGURE 1 Experimental setup for the measurement of the transmission intensity I_{out} through the FLC cell with linear feedback as a function of input light intensity I_{in}. F denotes the feedback gain ($V_a = V_b + FI_{out}$). For SSFLC, the cell is placed between polarizers.

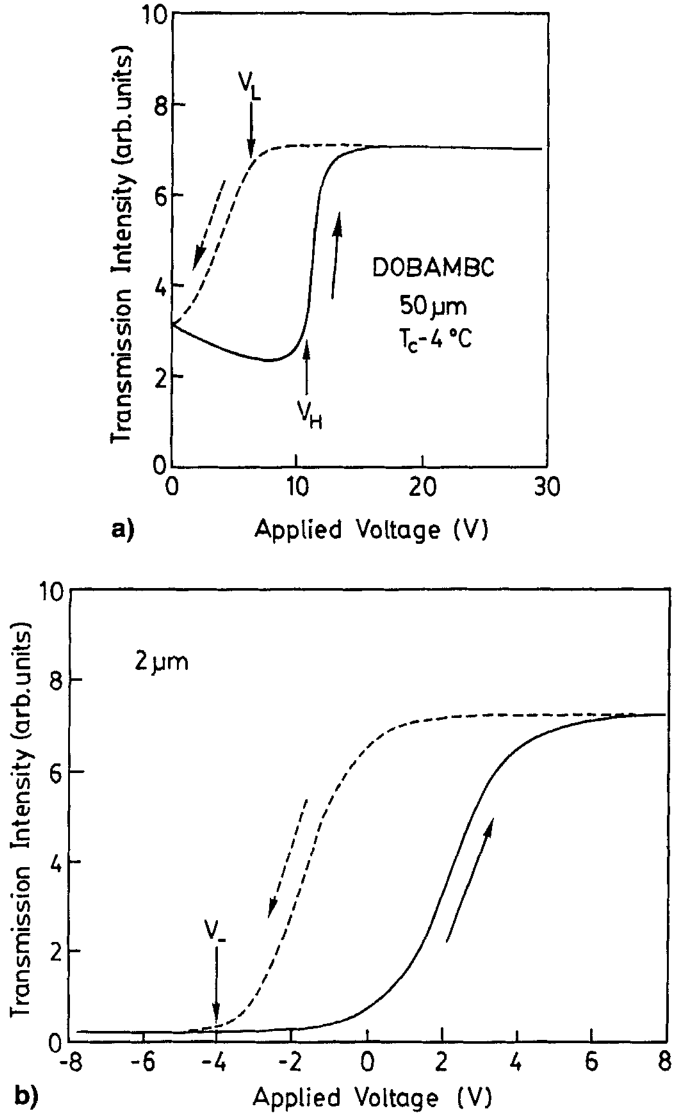

FIGURE 2 Typical voltage dependences of the transmission intensity in DHS (a) and SSFLC (b) cells. Solid and dashed lines describe increasing and decreasing cycles of the applied voltage, respectively.

voltage above the threshold voltage V_H, the transmission intensity increases accompanied with the unwinding of the helical structure, which results in the high transmission state (a solid line). Once the high transmission state is established, even with decreasing voltage below V_H, this state remains until the second threshold voltage V_L ($<V_H$) as shown with a dashed line in Figure 2(a). As a result, the hysteresis of the transmission intensity is observed.

The output intensity I_{out} through the DHS cell with a positive feedback gain is shown in Figure 3 as a function of input intensity I_{in}. The magnitude of bias voltage

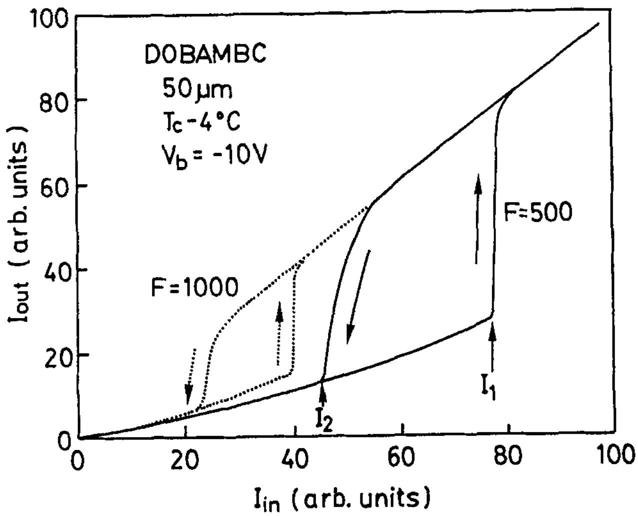

FIGURE 3 Typical I_{in}-I_{out} curves in DHS cell with various positive feedback gains ($F > 0$).

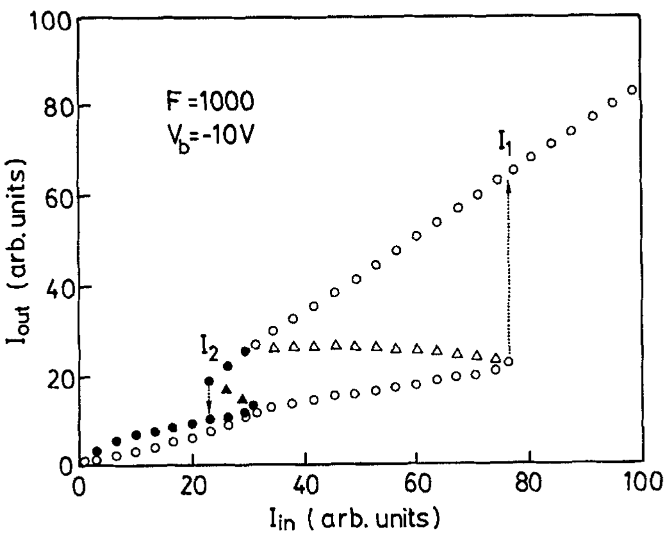

FIGURE 4 Typical I_{in}-I_{out} curves calculated from the $T(V_a)$ curve shown in Figure 2(a) and Equation (2). The open and closed circles correspond to increasing and decreasing stages in the $T(V_a)$ curve (Figure 2(a)), respectively.

is lower than the threshold voltage V_H of the transmission intensity hysteresis in Figure 2(a), and the polarity is negative. At low I_{in} the helical structure is wound, and the transmittance is low. With increasing I_{in}, the applied voltage increases, turning into the high transmission state with a threshold I_1. When I_{in} is decreased from the high transmission state, the voltage is reduced and the transmittance is lowered, resulting in the further reduction of the voltage. At the threshold intensity

I_2 ($I_2 < I_1$), I_{out} is decreased abruptly. That is, the optical bistability is realized for positive feedback gain. The optical hysteresis loop observed with a different feedback gain is also shown in Figure 3. With increasing feedback gain, the hysteresis loop becomes smaller and shifts toward lower intensity.

In the linear feedback system, the applied voltage V_a is expressed by

$$V_a = V_b + FT(V_a)I_{in}, \tag{1}$$

where F is the feedback gain and $T(V_a)$ is the transmittance which is a function

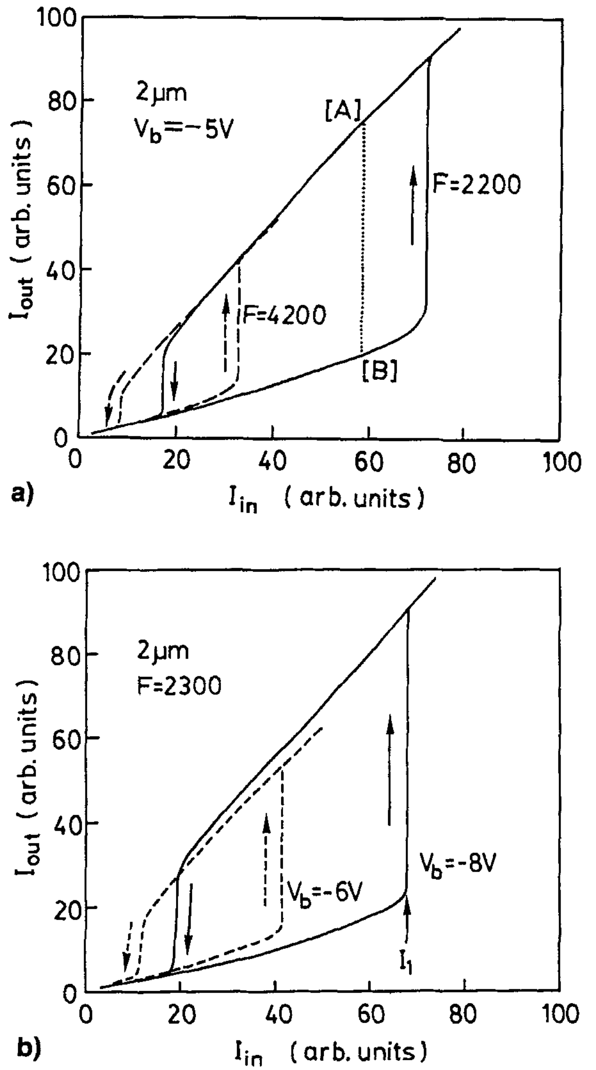

FIGURE 5 Typical I_{in}-I_{out} curves in SSFLC cell with positive feedback gain ($F > 0$) as a function of feedback gain F (a) and bias voltage V_b (b).

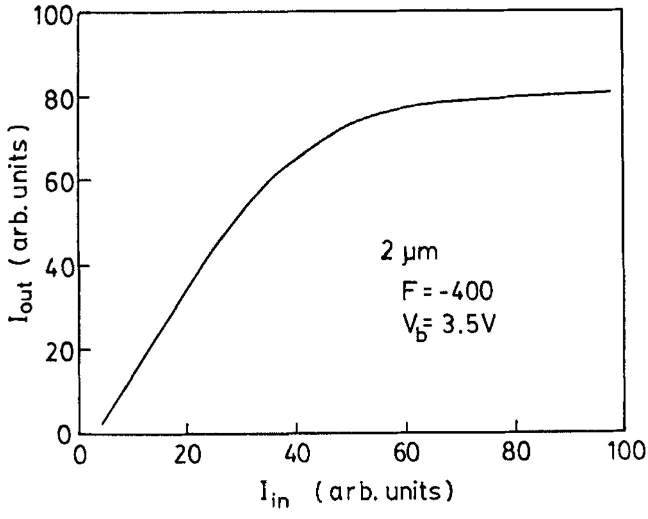

FIGURE 6 Typical I_{in}-I_{out} curve in SSFLC cell with negative feedback gain ($F < 0$).

of V_a, as shown in Figure 2(a). One can rewrite Equation (1) as

$$T(V_a) = (V_a - V_b)/FI_{in}. \tag{2}$$

Therefore, for a given input intensity I_{in}, the steady-state operating point with a linear feedback is determined by one of the intersections of the $T(V_a)$ curve shown in Figure 2(a) and the straight line given by Equation (2). This leads to the bistable loops of output versus input light intensity.

The calculated loops of output-versus-input light intensities for positive feedback are shown in Figure 4. It should be noted in this figure that two hysteresis exist. These hysteresis correspond to increasing and decreasing cycles of the transmission hysteresis shown in Figure 2(a). By the simulation with the increasing cycle in the $T(V_a)$ curve (a solid line in Figure 2(a)), the open circles in Figure 4, which determined the higher threshold I_1 in the experimentally observed bistable loop in Figure 3, were obtained. In the case of the calculation with the decreasing cycle in the $T(V_a)$ curve (a dashed line in Figure 2(a)), the closed circles in Figure 4, which determined the lower threshold I_2 in Figure 3, were obtained. Therefore, the hysteresis in the $T(V_a)$ curve characteristic to the FLC contributes to the expansion of the bistable region.

The optical limiting was also observed in the DHS cell with a negative feedback gain. In this case the bias voltage V_b was higher than V_H. At low input light intensities, since the voltage applied to the cell (V_a) is higher than threshold voltage V_H, the helical structure is unwound and the transmittance is high. Then, I_{out} increases in proportion to I_{in}. As I_{in} increases, V_a decreases, and transmittance decreases, resulting in the saturation of I_{out}. With increasing negative feedback gain, the range where I_{out} is proportional to I_{in} becomes narrow.

3.2 Feedbacked SSFLC

Voltage dependence of the transmission intensity of the light through the SSFLC cell is shown in Figure 2(b). The hysteresis loop which is caused by the bistability of the molecular orientation in SSFLC is observed. In this case sample cell was placed between crossed polarizers to obtain the extinction condition at negative voltage.

Figure 5 shows the I_{in}-I_{out} curve in the SSFLC cell with a positive feedback gain. The bias voltage V_b is lower than the threshold voltage V_- of the transmission intensity hysteresis in Figure 2(b). The optical bistability is also observed in the SSFLC cell with positive feedback gain in the same manner as the feedbacked DHS cell. With increasing feedback gain, the hysteresis loop becomes smaller and shifts toward lower intensity. Figure 5(b) shows the I_{in}-I_{out} curves in the SSFLC cell as a function of V_b. With increasing the magnitude of V_b, the threshold light intensity

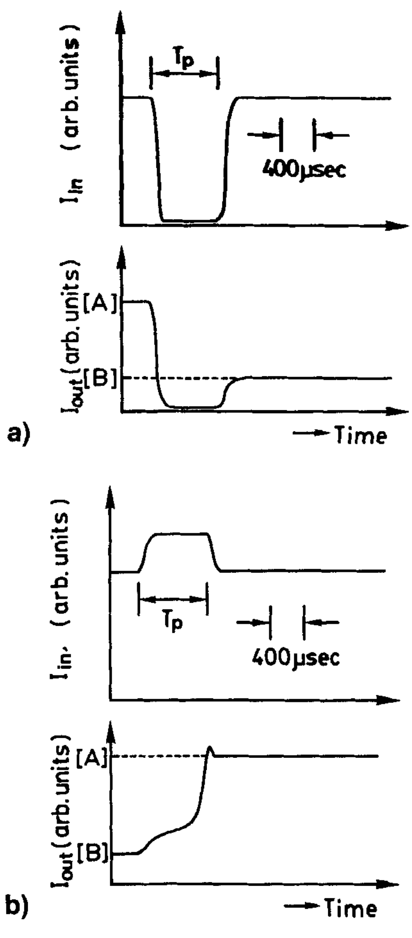

FIGURE 7 Dynamic responses of transmission intensity through the feedbacked SSFLC cell by pulse incidence light. (a) Switching from [A] to [B] states, (b) switching from [B] to [A] states.

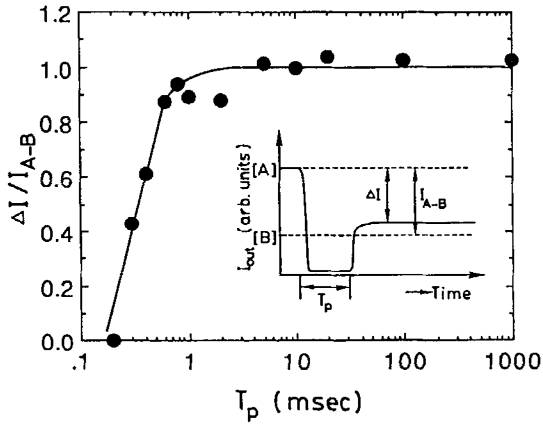

FIGURE 8 The dependence of $\Delta I/I_{A\text{-}B}$ on T_p. ΔI is the change of I_{out} from that in the [A] state by shutting off I_{in}. $I_{A\text{-}B}$ exhibits the difference of I_{out} between [A] and [B] states.

I_1 of the hysteresis loop shifts toward higher intensity. If the bias voltage V_b is too high, the applied voltage V_a after the transition to the on state at I_1 is too high.

Figure 6 shows I_{out} through a SSFLC cell with a negative feedback gain as a function of I_{in}. The optical limiting was also observed in the SSFLC cell. It should be noted that the optical bistability can be realized even with a negative feedback gain due to the hysteresis in the voltage dependence of the transmission intensity.

The switching between two stable states, [A] and [B], in Figure 5(a) can be realized by the control of the incident light. Figure 7 shows the typical response of I_{out} to the incident light pulse. The on state [A] turns into the off state [B] by shutting off the incident light instantaneously (Figure 7(a)). On the other hand, the off state [B] switches to the on state [A] by superimposing the light pulse on the incident light (Figure 7(b)). The switching can be realized with a short pulse width T_p of incident light pulse.

Figure 8 shows $\Delta I/I_{A\text{-}B}$ as a function of the T_p. ΔI is the change of I_{out} from that in the [A] state by shutting off I_{in} during T_p. $I_{A\text{-}B}$ is the differrence of I_{out} between [A] and [B] states. $\Delta I/I_{A\text{-}B} = 1$ shows the realization of the bistable switching from [A] to [B] states, while zero means that the switching is not carried out. It should be noted that the intermediate state between [A] and [B] is observed at short pulse width T_p. This is explained as follows. The pulse width T_p is too short to reorient completely the director of liquid crystal molecules in SSFLC cell. The high transmission state does not turn into complete extinction state in the voltage dependence of transmission intensity shown in Figure 2(b). As the result, when I_{in} is restored, the V_a increases again with the transmittance keeping intermediate state. Therefore, the intermediate I_{out} is observed in I_{in}-I_{out} curve.

4. SUMMARY

Hybrid optical bistability in smectic ferroelectric liquid crystal using the DHS and SSFLC electro-optical effects with linear electrical feedback was demonstrated.

Optical limiting and bistability were observed for the case of negative and positive feedback parameters, respectively. It was also found that the transmission hysteresis characteristic to the ferroelectric liquid crystal contributed to the exansion of the bistable region and to the realization of the bistability with a negative feedback gain. In the feedbacked SSFLC cell, dynamic switching between bistable states was observed at a short pulse width of the incident light.

References

1. I. C. Khoo, *Appl. Phys. Lett.*, **41**, 909 (1982).
2. M. M. Cheung, S. D. Durbin and Y. R. Shen, *Opt. Lett.*, **8**, 39 (1983).
3. J. Y. Kim and P. Palffy-Muhoray, *J. Appl. Phys.*, **66**, 362 (1989).
4. K. Yoshino, K. G. Balakrishnan, T. Uemoto, Y. Iwasaki and Y. Inuishi, *Jpn. J. Appl. Phys.*, **17**, 597 (1978).
5. Y. Iwasaki, K. Yoshino, T. Uemoto and Y. Inuishi, *Jpn. J. Appl. Phys.*, **18**, 2323 (1979).
6. N. A. Clark and S. T. Lagerwall, *Appl. Phys. Lett.*, **36**, 899 (1980).
7. K. Yoshino and M. Ozaki, *Jpn. J. Appl. Phys.*, **23**, L385 (1984).
8. S. Kishio, M. Ozaki, K. Yoshino and A. Sakamoto, *Mol. Cryst. Liq. Cryst.*, **144**, 43 (1987).
9. M. Ozaki, S. Kishio and K. Yoshino, *Jpn. J. Appl. Phys.*, **26**, Suppl. 26-2, 110 (1987).